

Multipath Delay Profile Acquisition for Ultra-Wideband PPM Systems

Dana Porrat, *Member, IEEE*, and Urbashi Mitra, *Fellow, IEEE*

Abstract—The acquisition of a multipath channel profile (including the leading delay) for ultra-wideband pulse position modulation (PPM) communication systems is considered in the limit of large bandwidth. Optimal acquisition is defined by the maximum likelihood detector whose performance can be assessed via order statistics. Four channel scenarios are examined: deterministic or Gaussian channel taps, uniform or exponential power delay profiles. For these four channels, the rate of growth of the multipath as a function of bandwidth which leads to acquisition failure is determined. Acquisition is not even partially possible on multipath channels with deterministic path amplitudes, if the number of paths diverges too fast. Furthermore, if the number of independent Gaussian paths increases without bound, but slower than the bandwidth, then the system cannot even partially acquire in the limit. These negative results are shown for somewhat idealized environments, implying that multipath delay profile acquisition will fail under more realistic conditions.

Index Terms—Channel uncertainty, multipath channels, order statistics, pulse position modulation (PPM), ultra-wideband (UWB), wideband communications.

I. INTRODUCTION

ULTRA-wideband (UWB) impulsive systems have gained recent interest for communications, as well as channel imaging and positioning. While significant diversity is achievable given the large amount of multipaths in UWB channels, methods for harnessing such diversity when the channel is unknown remain a challenge. In fact, the fundamental limits of UWB signaling in the presence of channel uncertainty have not been fully established. In this paper, we consider a specific form of channel uncertainty: unknown multipath delay profile. In particular, we assess the challenge of learning the multipath delay profile in the limit of large bandwidth in the context of pulse position modulation (PPM) systems. Our main contribution is a negative conclusion: acquisition of the delay profile cannot be even partially achieved, even if all system resources are devoted to estimating the delays of the multipath.

While our approach is based on detection theory, we are informed by prior information theoretic approaches which endeavor to establish the capacity of wideband communication in the limit of large bandwidth [12], [17], [20], [23], [31], [32],

Manuscript received December 4, 2006; revised June 1, 2007. The associate editor coordinating the review of this manuscript and approving it for publication was Prof. Zengyuan Xu.

D. Porrat is with the Hebrew University, Jerusalem, Israel (e-mail: dporrat@cs.huji.ac.il).

U. Mitra is with the University of Southern California, Los Angeles, CA 90089 USA (e-mail: ubli@ucs.edu).

Color versions of one or more of the figures in this paper are available online at <http://ieeexplore.ieee.org>.

Digital Object Identifier 10.1109/JSTSP.2007.907489

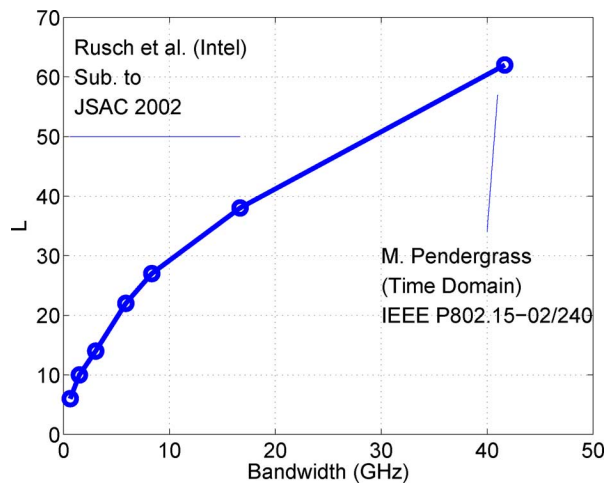


Fig. 1. Number of significant channel paths versus bandwidth. The paths accounting for 60%–90% of the energy were counted in two separate measurement campaigns. The Intel data were taken from [27] and the time-domain data from [21].

[34]. Several observations can be drawn from these works: unknown path delays have a more significant impact on wideband capacity than unknown path amplitudes and flash signaling can sometimes counteract the effects of channel uncertainty in the wideband limit. We examine flashy PPM systems and ask what is the maximum rate of growth of the multipath as a function of bandwidth which enables acquisition of the multipath delay profile. Recent wideband channel-propagation measurements suggest that the number of channel paths grows with bandwidth, an almost linear rate is reported by [29], and a sublinear rate is shown in [23] and [28] (see Fig. 1). Flash signaling enables spread-spectrum signaling to achieve channel capacity even in the presence of an unknown multipath delay profile so long as the rate of growth of the multipath with increasing bandwidth is not too large. However, flash signaling does not appear to comparably assist PPM. An intuitive interpretation of our results is as follows: the relatively low spectral efficiency of PPM does not allow strongly bursty (very flashy) signaling which is necessary to overcome the noncoherent nature of the channel, in contrast to direct-sequence spread-spectrum signaling.

Knowledge of path delays is essential for proper operation of PPM systems, and timing errors seriously degrade PPM system performance [19], [33] as well as that of spread-spectrum systems (see [5] and references therein). The relatively low power per Hertz considered for UWB systems implies that it is necessary to acquire a significant subset of the multipath delay profile to ensure reasonable energy capture; however, in practice, not all paths are acquired for complexity reasons [36] and thus

a “selective RAKE” is implemented. Classical UWB channel synchronization is often performed by a correlation operation followed by a threshold decision [9], [13], [15], [37]. We have shown that in the limit of large bandwidth, threshold synchronization fails [22]. A similar conclusion is drawn in [35]¹ for high SNR. We observe that there has been significant interest in determining high performance channel estimation methods for both the channel taps as well as the multipath delay profile for UWB systems [2]–[4], [11], [14], [18]. In providing a result for a simple system, we do not treat some of the practical aspects considered in this prior work; however, as it is a negative result, our work implies that multipath delay profile acquisition for flashy PPM in the limit of large bandwidth is not possible for practical systems.

We assume all system resources are devoted to training, the use of guard bands to avoid inter-symbol interference and no pulse distortion [8], [25], [26]². We consider several channel models based on uniform or exponentially decaying energy profiles and deterministic or Gaussian distributed channel tap coefficients, in contrast to [20], [23], and [32], which considered only uniform energy profiles. The objective is to consider mathematically tractable models which still capture key features of real UWB channels. Thus the “sparse” nature of multipath profiles (presence of nonzero taps due to clustering [7], [10]) and nonuniform multipath delay profiles (e.g., [7]) are both captured within our family of examined channels. Consistent with [23] and [32], we consider a scenario with an average power constraint per transmitted symbol. For narrowband systems, the Gaussian model for channel taps is derived from invoking the Central Limit Theorem (see e.g., [24]); it is not clear whether such arguments can be made for the UWB case [38] as the number of paths which can be combined within a resolution bin may decrease as a function of increasing bandwidth. However, we believe such models can still provide useful intuition for real systems.

Our method of proof is based on exploiting properties of uniform energy multipath profiles for both the deterministic and Gaussian scenarios. For these two cases, the maximum likelihood multipath delay acquisition algorithm can be cast into a method based on order statistics [6]. We show that in the limit of large bandwidth (W), it is impossible to acquire the delay corresponding to the path with the largest magnitude and thus we cannot acquire any of the path delays. The exponential delay profiles cases are treated by examining a corresponding uniform delay profile case which provides performance superior to that of the exponential profile case. When acquisition fails for the corresponding uniform profile, it also fails for the exponential profile. We examine regimes where the bandwidth diverges $W \rightarrow \infty$ and the number of multipaths (L) also grows without bound $L \rightarrow \infty$. For both deterministic profiles if $L < W^\rho$ where $\rho \approx 1/2$, acquisition fails. For the Gaussian profiles, the condition $L/W \rightarrow 0$ ensures that the multipath delay profile cannot be acquired. We emphasize that acquisition fails for any growth rate lower than that specified above. In particular note

that for $\rho \approx 1/2$, the implication is that multipath that grows logarithmically with bandwidth also results in an acquisition failure.

Our results show that for many cases of interest, the receiver will be unable to acquire the multipath delay profile at large bandwidths. The implication of these results for achievable rates of noncoherent PPM systems is consistent with the numerical analysis of [30], which suggests that the communication rate decreases as the bandwidth increases. Direct-sequence spread-spectrum systems operating over a channel with a uniform power delay profile, with multipath delay profile knowledge at the receiver, achieve the channel capacity in the limit if $L/W \rightarrow 0$, but without this knowledge the condition becomes $L \log W/W \rightarrow 0$. For PPM, the effect of knowledge of the path delays converts the conditions for achieving capacity from $L/\log W \rightarrow 0$ with knowledge of the delays to $L \sim \text{const}$, or possibly a decreasing number of multipath, without this knowledge. Thus, the knowledge of the path delays enables the removal of a factor of $\log W$ from the rate of increase of the number of paths which allows the system to achieve the channel capacity [23]. The underlying reasoning is that with L i.i.d. paths, the amount of information needed to describe the channel path delays is $L \log W$. This information cannot be applied to the system’s achievable rate for communication.

This paper is organized as follows: Section II describes the transmitted signal, channel model and received signal. The optimal receiver is discussed in Section III along with preparatory calculations. The main results, for channels with a uniform and an exponential power delay profile, are provided in Sections IV and V. Discussion of the result and final conclusions are presented in Section VI. The Appendix derives a simple equivalent form of the maximum likelihood multipath profile acquisition algorithm for the case of uniform energy profile for Gaussian channel coefficients.

II. SIGNAL MODEL

A. Transmitted Signal

We consider power limited PPM, where the transmitted signal is a concatenation of symbols of the type

$$p\left(t - \frac{1}{W}b\right) \quad t \in [0, T_s) \quad \text{where } p(t) = \begin{cases} \sqrt{\frac{\mathcal{E}}{\theta}}, & t \in [0, \frac{T_s}{N}) \\ 0, & \text{else} \end{cases} \quad (1)$$

The symbol duration is given by T_s and the number of pulse positions is dictated by the transmission bandwidth W . The data symbol is denoted $b \in \{0, 1, \dots, N-1\}$ where $N = WT_s$. The average transmitted energy per symbol is \mathcal{E} —it is bandwidth independent and ensures an average power constraint. The entire transmitted waveform (multiple symbols) is denoted by $x(t)$. We shall assume that the symbol duration does not diminish with increasing bandwidth.

The flash parameter θ in (1) controls the duty cycle of communications. With the use of flash signaling, transmission is bursty and communication occurs over a fraction θ of the total communication period. During the active periods, symbols of

¹The same authors offer a review of UWB channel acquisition in [1].

²We observe that maximum-likelihood based channel estimation methods with proper channel modeling exhibit robustness to pulse distortion which is unknown at the receiver as we have shown in [3].

the type (1) are used and at other times the transmitter is silent. θ is known at the receiver and furthermore, the receiver is aware of the on-periods of communication. Note the distinction between flashy transmission and PPM modulation. For regular data transmission, the receiver must detect which one of the $N = WT_s$ pulse positions has been employed in each symbol; in contrast, with flashy transmission, the receiver is synchronized to the on-periods of communication. We note that if θ is small, then the transmitter is predominantly silent. We require a positive (nondiminishing) data rate with increasing bandwidth. Thus, the parameter θ must be large enough so that $\theta \log W$ does not diminish, since the data rate with flash signaling is proportional to $\theta \log_2 WT_s$. The requirement on θ can be written as

$$\theta \geq \frac{k_1}{\log(Wk_2)} \quad (2)$$

with fixed k_1, k_2 that are independent of the bandwidth.

Several features of our setup should be underscored. The first is that there is no constraint imposed on the number of PPM positions that are employed for data signaling. Thus, a guard time can be implemented by limiting the positions employed. Second, we emphasize the employment of a lower bounded symbol time, where the lower bound does not depend on the signal bandwidth. We do not consider schemes where the symbol time diminishes with bandwidth. Thus, the number of bits that can be transmitted in a single coherence period (that is equivalent to the spectral efficiency) depends logarithmically on the bandwidth. Note that systems that use a guard period between symbols that depends on the channel path delays, have a natural lower bound on their symbol time.

B. The Channel

We assume a tapped delay line model for the channel $h(t)$, thus

$$h(t) = \sum_{l=1}^L g_l \delta\left(t - \frac{d_l}{W}\right)$$

where the channel amplitudes are given by g_l , $\delta(\cdot)$ denotes the Dirac delta function and $\{d_l\}$ represent the path delays which are assumed non-negative integers between 1 and M . We assume an average power constraint: $\mathbf{E} \left[\sum_{i=1}^L g_i^2 \right] = 1$.

The maximal possible number of resolvable paths is given by $M = WT_d$, where T_d represents the delay spread of the channel, and thus the number of multipath L satisfies $L \leq M$. Given M possible values of the path delays, we assume that the realizations of the path delays are uniformly distributed over $\binom{M}{L} = M!/(L!(M-L)!)$ possibilities. Note that our description is general in that the leading delay is unknown. The channel model is of the block-type: the channel is fixed over the channel coherence time T_c ; channel realizations at different coherence periods are statistically independent. Channel variation over time is immaterial to our results, that hold as long as the average power per channel realization is finite and the channel is static over finite lengths of time.

In the sequel, we shall consider four different channel types which differ in their path amplitude model (deterministic versus

random) and in their profile (uniform power delay profile and exponential delay profile). As such, we treat a large class of channels. While specific practical channel models as specified in the IEEE 802.15 standard are not exactly examined, many of the key features are considered herein such as ‘‘sparse’’ channels and those with a decaying power delay profile. We begin with an explicit treatment of the deterministic uniform delay profile case as the proof technique is easily illustrated. Key differences between the deterministic and random uniform delay profile scenarios are outlined. For the remaining exponential delay profile cases, the deterministic case is sketched out and the explicit proof for the random case is provided.

To highlight the differences between the four channel models, we list the statistics of their channel taps as follows:

- (ud) uniform (u) average power delay profile, with equal and deterministic (d) path amplitudes

$$g_l^{(\text{ud})} = \frac{1}{\sqrt{L}} \quad l = 1, \dots, L \quad (3)$$

- (ur) uniform (u) average power delay profile, with random (r) i.i.d. Gaussian path amplitudes

$$g_l^{(\text{ur})} \sim \mathcal{N}\left(0, \frac{1}{L}\right) \quad l = 1, \dots, L \quad (4)$$

- (ed) exponential (e) average power delay profile, with deterministic (d) path amplitudes, that depend on the delay

$$g_l^{(\text{ed})} = \frac{F^{(\text{e})}}{\sqrt{L}} e^{-d_l T_d / M \tau} \quad l = 1, \dots, L$$

$$\text{where } F^{(\text{e})} = \sqrt{M \frac{1 - e^{-2T_d / M \tau}}{1 - e^{-2T_d / \tau}}} e^{T_d / M \tau} \quad (5)$$

note that $F^{(\text{e})}$ is a normalization constant such that $\sum_{l=1}^L g_l^{(\text{ed})2} = 1$. The variable τ controls the decay rate of the profile. Recall that the d_l are the path delays.

- (er) exponential (e) average power delay profile, with random (r) Gaussian path amplitudes

$$g_l^{(\text{er})} \sim \mathcal{N}\left(0, \sigma_l^{(\text{er})2}\right) \quad l = 1, \dots, L$$

$$\text{with } \sigma_l^{(\text{er})2} = \frac{F^{(\text{e})2}}{L} e^{-2d_l T_d / M \tau} \quad \text{and } F^{(\text{e})} \text{ is as above.} \quad (6)$$

The notation (ud), (ur), (ed), and (er) is used throughout to denote the four channel models.

C. Received Signal

The received signal is given by

$$\begin{aligned} y(t) &= h(t) \otimes x(t) + z(t) \\ &= \sum_{l=1}^L g_l x\left(t - \frac{d_l T_d}{M}\right) + z(t), \end{aligned}$$

where $z(t)$ is a zero-mean, unit variance, white Gaussian noise process. At the receiver, the received signal is pulse matched filtered and sampled at $1/W$ yielding the following discrete-time equivalent signal:

$$Y_i = \sum_{l=1}^L g_l X_{i-d_l} + Z_i \quad (7)$$

where

$$X_i = \begin{cases} \sqrt{\frac{\mathcal{E}}{\theta}} & \text{if } \exists n : i \div N = n \text{ and } i \bmod N = b[n] \\ 0 & \text{else} \end{cases} \quad i = 1, \dots, T_c W$$

$i \div N = n$ signifies the largest integer n such that $nN \leq i$, the condition $i \div N = n$ means that the n^{th} PPM symbol is chosen. $b[n]$ is the value of the n^{th} symbol. The signal X_i is zero-valued except at the positions corresponding to the transmitted PPM pulse; recall that $N = WT_s$ is the number of positions within a symbol. $b[n]$ indicates the position chosen for the n^{th} symbol. The noise samples $\{Z_i\}$ are zero-mean with unit variance, and the average signal to noise ratio is given by \mathcal{E} .

In order to assess the challenges of acquisition of PPM in multipath, we analyze a further simplified system. We assume no intersymbol interference (achieved, for example by using a guard time) and knowledge of the PPM symbols (training). Under these idealized conditions, we show a failure to acquire, implying statements about more practical systems.

Given our assumptions about the channel noise and the multipath coefficients, each observation sample is Gaussian. If we define $\overline{\mathbf{MP}}$ as the event that a multipath component is present at a sample of the received signal and $\overline{\overline{\mathbf{MP}}}$ is the complementary event, that is the event of noise only, then under the four channel models, we have $Y_i^{(xx)} | \overline{\mathbf{MP}} \sim \mathcal{N}(m_i^{(xx)}, v_i^{(xx)})$, where

$$\begin{aligned} m_i^{(\mathbf{ud})} &= \sqrt{\frac{\mathcal{E}}{\theta L}} & m_i^{(\mathbf{ur})} &= 0 \\ m_i^{(\mathbf{ed})} &= \sqrt{\frac{\mathcal{E}}{\theta}} g_i^{(\mathbf{ed})} & m_i^{(\mathbf{er})} &= 0 \\ v_i^{(\mathbf{ud})} &= 1 & v_i^{(\mathbf{ur})} &= \frac{\mathcal{E}}{\theta L} + 1 \\ v_i^{(\mathbf{ed})} &= 1 & v_i^{(\mathbf{er})} &= \frac{\mathcal{E}}{\theta} \sigma_i^{(\mathbf{er})^2} + 1 \end{aligned} \quad (8)$$

$Y_i | \overline{\overline{\mathbf{MP}}} \sim \mathcal{N}(0, 1)$ and $i = 1, \dots, M$.

Given that we know the PPM symbol, the observation vector is of length M and of the M possible positions, L correspond to the multipath. The remaining $M - L$ positions correspond to noise.

III. MAXIMUM LIKELIHOOD ACQUISITION

Recall that the position of the transmitted PPM symbol is known; however, the initial multipath delay and multipath profile are unknown. The acquisition problem can be posed as a multiple hypothesis testing problem for which there are $\binom{M}{L}$

hypotheses $\{H_q\}$ with L non-zero channel taps out of M possible positions. The received signal under each hypothesis can be written as a vector of length M

$$\underline{Y}^0 | H_q = \sqrt{\frac{\mathcal{E}}{\theta}} \underline{s}_q^0 + \underline{Z} \quad (9)$$

where $\underline{Z} \sim \mathcal{N}(\underline{0}, \mathbf{I})$ and $q = 1, \dots, \binom{M}{L}$

$$\underline{s}_q^0 = \left[\underbrace{0, \dots, g_1^0, 0, \dots, g_2^0, \dots, g_L^0, \dots, 0}_{L \text{ amplitudes at corresponding delays}} \right]^T \quad (10)$$

To facilitate the description of the optimal, maximum likelihood (ML) detector we define the multipath location vector, that is, for each particular multipath profile vector \underline{s}_q^0 , we have an M long vector

$$\underline{p}_q = \left[\underbrace{0, \dots, 1, \dots, 1, \dots, 1}_{L \text{ ones at corresponding delays}} \right]^T \quad q = 1, 2, \dots, \binom{M}{L}. \quad (11)$$

For both the **(ud)** and **(ed)** scenarios, the ML detector is a correlator

$$\hat{q}^{(\mathbf{ud}),(\mathbf{ed})} = \arg \max_q \underline{s}_q^{(\mathbf{ud}),(\mathbf{ed})T} \underline{Y}^{(\mathbf{ud}),(\mathbf{ed})}. \quad (12)$$

Due to the fact that the signal vectors in the **(ud)** case are equal energy and each non-zero path has equal amplitude, the maximum likelihood **(ud)** detector is a simplified correlator structure

$$\hat{q}^{(\mathbf{ud})} = \arg \max_q \underline{p}_q^T \underline{Y}^{(\mathbf{ud})}. \quad (13)$$

Given the form of \underline{p}_q , we can see the following equivalence. Let $Y_{1:M}, Y_{2:M}, \dots, Y_{L:M}$ be the L largest components of \underline{Y} . The most likely multipath profile is the one that corresponds to the delays of these components, thus

$$\max_q \underline{p}_q^T \underline{Y} = \sum_{j=1}^L Y_{j:M}. \quad (14)$$

Thus the maximum likelihood detector is equivalent to determining the multipath locations by selecting the L positions/samples with the L largest signal values. This equivalence is critical as it enables the use of order statistics to analyze performance.

For the random path scenarios, **(ur)** and **(er)**, the ML detector is an energy detector. This is due to the fact that the vector observations are zero-mean Gaussian vectors with $M \times M$ covariance matrices, $C_q^{(\mathbf{ur}),(\mathbf{er})} = \mathbf{E} \left[\underline{s}_q^{(\mathbf{ur}),(\mathbf{er})} \underline{s}_q^{(\mathbf{ur}),(\mathbf{er})T} \right] + \mathbf{I}$

$$\begin{aligned} & \arg \max \text{Prob}(\underline{Y}^{(\mathbf{ur}),(\mathbf{er})} | H_q) \\ &= \arg \max \frac{1}{\sqrt{\det C_q^{(\mathbf{ur}),(\mathbf{er})}}} \\ & \exp -\frac{1}{2} \underline{Y}^{(\mathbf{ur}),(\mathbf{er})T} C_q^{(\mathbf{ur}),(\mathbf{er})^{-1}} \underline{Y}^{(\mathbf{ur}),(\mathbf{er})}. \end{aligned} \quad (15)$$

For the (\mathbf{ur}) case in particular, we have $C_q^{(\mathbf{ur})} = (\mathcal{E}/L\theta)\text{diag}(\underline{p}_q) + \mathbf{I}$ $q = 1, \dots, \binom{M}{L}$. And thus the detector simplifies to

$$\arg \max \text{Prob}(\underline{Y}^{(\mathbf{ur})} | H_q) = \arg \min \underline{Y}^{(\mathbf{ur})T} C_q^{(\mathbf{ur})^{-1}} \underline{Y}^{(\mathbf{ur})} \quad (16)$$

which follows from the fact that $\det C_q^{(\mathbf{ur})} = (1 + \mathcal{E}/L\theta)^L \forall q$.

After some manipulation (see the Appendix), it can be shown that the ML detector is equivalent to

$$\hat{q}^{(\mathbf{ur})} = \arg \max_q \underline{p}_q^T \left| \underline{Y}^{(\mathbf{ur})} \right| \quad (17)$$

where $|\underline{Y}^{(\mathbf{ur})}|$ is a vector whose components correspond to the absolute values of the components of the vector $\underline{Y}^{(\mathbf{ur})}$. With this perspective of the maximum likelihood detector, we can develop a method for evaluating the likelihood of an error through order statistics. In order to upper-bound the detection performance in the exponential power delay profile (PDP) case, we analyze a specific uniform PDP; the acquisition performance of this profile bounds that of the exponential PDP.

In analyzing the random path amplitudes, we apply order statistics on the signed values $\{Y_i^{(\mathbf{ur})}\}$ rather than the absolute values, $\{|Y_i^{(\mathbf{ur})}|\}$. The final result is shown by exploiting the symmetry of the order statistics about the mean [6] and noting that if the highest positive signal position is dominated by noise, then the lowest negative signal position is also dominated by noise, in the sense that the noise is more negative.

The proofs of the four theorems are very similar, they follow from simple observations of the events leading to an error for the maximum likelihood detector over a channel with a uniform PDP. We consider the particular error event where none of the paths are correctly detected. For this error event, we show that with reasonable growth rates on L versus M , its probability is unity in the limit of large L and M . As M is proportional to the bandwidth of the system, we ultimately obtain a large bandwidth result which shows that multipath delay profile acquisition is not possible for channels where the effective number of paths grows with the bandwidth.

A. Key Formulas From Order Statistics

We next review useful formulas on order statistics that will be employed repeatedly in the proofs of our results. From Cramér's book [6, Section 28.6] we have the mean and variance of the order statistics of Gaussian variables. We order G identically and independently distributed Gaussians with mean m and variance σ^2 . The ν^{th} variable from the top, with $\nu \leq G/2$, has mean

$$\mathbf{E}_{\nu:G} = m + \sigma \left(\frac{\sqrt{2 \ln G} - \ln \ln G + \ln 4\pi + 2(A_1(\nu) - C)}{2\sqrt{2 \ln G}} + O\left(\frac{1}{\ln G}\right) \right) \quad (18)$$

and variance

$$\text{var}_{\nu:G} = \frac{\sigma^2}{2 \ln G} \left(\frac{\pi^2}{6} - A_2(\nu) \right) + O\left(\frac{1}{\ln^2 G}\right) \quad (19)$$

where $C \approx 0.5772$ is Euler's constant, and for $\nu > 1$

$$A_1(\nu) = \sum_{s=1}^{\nu-1} \frac{1}{s} \approx \int_1^{\nu} \frac{1}{x} dx = \ln \nu \quad (20)$$

$$A_2(\nu) = \sum_{s=1}^{\nu-1} \frac{1}{s^2}. \quad (21)$$

Note that $A_2(\nu) \leq \pi^2/6$. In fact, $A_2(\nu) \xrightarrow{\nu \rightarrow \infty} \pi^2/6$ as shown by Euler. For $\nu = 1$ (the largest of the G variables), we have from [16, Sec. 21-4]: $A_1(1) = A_2(1) = 0$.

The moments of the order statistics with $\nu > G/2$ are symmetric around m [6], thus

$$\mathbf{E}_{\nu:G} = 2m - \mathbf{E}_{G-\nu+1:G} \quad (22)$$

$$= m - \sigma \left(\sqrt{2 \ln G} - \frac{\ln \ln G + \ln 4\pi + 2(A_1(\nu) - C)}{2\sqrt{2 \ln G}} + O\left(\frac{1}{\ln G}\right) \right) \quad (23)$$

$$\text{var}_{\nu:G} = \text{var}_{G-\nu+1:G} = \frac{\sigma^2}{2 \ln G} \left(\frac{\pi^2}{6} - A_2(\nu) \right) + O\left(\frac{1}{\ln^2 G}\right). \quad (24)$$

We next provide an application of these formulas to determine the statistics of the noise-only scenario, which is common to all four channel models considered.

B. L^{th} Largest Noise Variable

We show that the L^{th} largest of the noise variables equals $\sqrt{2 \ln(M-L)} - \ln L / \sqrt{2 \ln(M-L)}$ in the limit of large M , L , if $L \leq M/3$. We use (18) and (19) with $G = M - L$ random variables, and consider the $\nu = L$ largest variable, *i.e.*, there are $L - 1$ variables larger than the one we investigate. Recall that $m = 0$ and $\sigma = 1$, which yield the following mean for the variable of interest, that holds for $L \leq M/3$:

$$\mathbf{E}_{L:M-L} = \sqrt{2 \ln(M-L)} - \frac{\ln \ln(M-L) + \ln 4\pi + 2(A_1(L) - C)}{2\sqrt{2 \ln(M-L)}} + O\left(\frac{1}{\ln(M-L)}\right) \quad (25)$$

and variance

$$\text{var}_{L:M-L} = \frac{1}{2 \ln(M-L)} \left(\frac{\pi^2}{6} - A_2(L) \right) + O\left(\frac{1}{\ln^2(M-L)}\right). \quad (26)$$

We observe that $A_2(L)$ is finite for any L , thus $\lim_{L, M \rightarrow \infty} \text{var}_{L:M-L} = 0$. Therefore, in the limit of large M and L , the L^{th} largest variable approaches a constant that equals its mean.

To further investigate the mean, we employ the simple approximation above [see (21)] for $A_1(L)$, for large L , to achieve

$$\mathbf{E}_{L:M-L} \approx \frac{\sqrt{2 \ln(M-L)}}{\frac{\ln \ln(M-L) + \ln 4\pi + 2(\ln L - C)}{2\sqrt{2 \ln(M-L)}}} + O\left(\frac{1}{\ln(M-L)}\right) \quad (27)$$

$$\approx \sqrt{2 \ln(M-L)} - \frac{\ln L}{\sqrt{2 \ln(M-L)}}. \quad (28)$$

Observe that $\lim_{L,M \rightarrow \infty} \mathbf{E}_{L:M-L} = \infty$, and $\lim_{L,M \rightarrow \infty} \mathbf{var}_{L:M-L} = 0$. The L^{th} noise variable does not strictly converge in the mean-square sense because its mean is not defined; however, convergence in distribution to the constant mean is achieved.

IV. UNIFORM DELAY PROFILE

A. Deterministic Path Amplitudes

We begin by focusing on deterministic, uniform delay profile channels, and provide the following theorem:

Theorem 1: (ud) case. Consider M independent, Gaussian random variables with the following distributions:

$$Y_i^{(\text{ud})} \sim \mathcal{N}\left(\sqrt{k \frac{\log M}{L}}, 1\right), \quad i = 1, 2, \dots, L \quad (29)$$

$$Z_i \sim \mathcal{N}(0, 1), \quad i = 1, 2, \dots, M-L \quad (30)$$

k is a constant that does not depend on L or M ; $L \leq M/3$.

We order the $Y_i^{(\text{ud})}$ such that $B_{1:L}^{(\text{ud})} = \max Y_i^{(\text{ud})}$ and $B_{L:L}^{(\text{ud})} = \min Y_i^{(\text{ud})}$; similarly, $S_{1:M-L} = \max Z_i$, $S_{M-L:M-L} = \min Z_i$ and $S_{L:M-L}$ is the L^{th} largest of $\{Z_i\}_{1}^{M-L}$. Then

$$\lim_{M,L \rightarrow \infty} P\left[S_{L:M-L} > B_{1:L}^{(\text{ud})}\right] = 1 \quad \text{if } \frac{L}{M\rho} < c \text{ where } \rho = 4 - 2\sqrt{3} \text{ and } c < 1 \text{ is a constant.} \quad (31)$$

Proof: We first determine the mean of the largest signal variable, and show that this random variable converges to the mean in distribution in the limit of large M and L . We use (18) and (19) again, with $G = L$ random variables, and examine the largest variable, that is $\nu = 1$. Recall that $m = \sqrt{k(\log M/L)}$ and $\sigma = 1$, yielding the mean

$$\mathbf{E}_{1:L}^{(\text{ud})} = \sqrt{k \frac{\log M}{L}} + \sqrt{2 \ln L} - \frac{\ln \ln L + \ln 4\pi - 2C}{2\sqrt{2 \ln L}} + O\left(\frac{1}{\ln L}\right) \quad (32)$$

$$\approx \sqrt{k \frac{\log M}{L}} + \sqrt{2 \ln L} \quad (33)$$

where the latter statement follows for large L and $C \approx 0.5772$. The variance is

$$\mathbf{var}_{1:L}^{(\text{ud})} = \frac{1}{2 \ln L} \frac{\pi^2}{6} + O\left(\frac{1}{\ln^2 L}\right). \quad (34)$$

As in Section III-B, $\lim_{M,L \rightarrow \infty} \mathbf{E}_{1:L}^{(\text{ud})} = \infty$, and $\lim_{M,L \rightarrow \infty} \mathbf{var}_{1:L}^{(\text{ud})} = 0$. We wish to determine the conditions for which $\mathbf{E}_{L:M-L} > \mathbf{E}_{1:L}^{(\text{ud})}$. This goal is accomplished by manipulating (28) and (33) to yield the inequality below. We use \gg to indicate that the difference between the two sides is unbounded in the limit, and denote by $\gg?$ inequalities that we attempt to prove

$$\sqrt{2 \ln(M-L)} \gg? \sqrt{k \frac{\log M}{L}} + \sqrt{2 \ln L} + \frac{\ln L}{\sqrt{2 \ln(M-L)}}. \quad (35)$$

To facilitate this comparison, we compare each of the three terms on the right hand side of (35) with three terms of a decomposition of the left-hand side. That is, let

$$\sqrt{2 \ln(M-L)} = (\alpha + \beta + \gamma) \sqrt{2 \ln(M-L)} \quad \text{where } \alpha + \beta + \gamma = 1 \quad (36)$$

where α, β and γ are positive constants that are not functions of M and L . We next evaluate three comparisons. For the first term of (35), we square both sides of the inequality of interest

$$\alpha^2 2 \ln(M-L) \gg? k \frac{\log M}{L} \quad (37)$$

$$\alpha^2 2 \left(\ln M + \ln \left(1 - \frac{L}{M}\right) \right) \gg? k \frac{\log M}{L}. \quad (38)$$

The left-hand side of (38) dominates over the right hand side for any positive α , if $L, M \rightarrow \infty$ and $L/M < c$, for a constant $c < 1$.

For the second term of (35), we also square both sides, yielding

$$\beta^2 \ln(M-L) \gg? \ln L \quad (39)$$

$$(M-L)^{\beta^2} \gg? L \quad (40)$$

$$M^{\beta^2} \left(1 - \frac{L}{M}\right)^{\beta^2} \gg? L \rightarrow M^{\beta^2} \gg? L. \quad (41)$$

Examining the final term of (35)

$$\gamma \sqrt{2 \ln(M-L)} \gg? \frac{\ln L}{\sqrt{2 \ln(M-L)}} \quad (42)$$

$$\gamma 2 \ln(M-L) \gg? \ln L \quad (43)$$

$$(M-L)^{2\gamma} \gg? L \rightarrow M^{2\gamma} \gg? L. \quad (44)$$

We wish to consider the weakest constraints on L and M such that acquisition fails. Thus, we wish to maximize the smallest of $\{\beta^2, 2\gamma\}$. This implies that $\beta^2 = 2\gamma$.

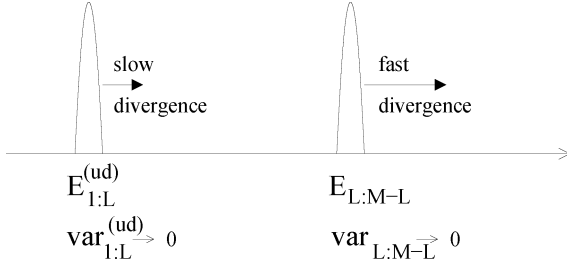


Fig. 2. Illustration of the distribution of the strongest signal position in the uniform PDP with deterministic amplitudes case (**ud**) and the L^{th} strongest noise position. Note that both variances diminish, while the mean of the L^{th} noise diverges faster than the mean of the strongest signal.

We next invoke our sum constraint: $\alpha + \beta + \gamma = 1$. Our first inequality holds for arbitrary α if $\lim_{L,M \rightarrow \infty} (L/M) < c < 1$. Thus, solving the quadratic equation: $\beta + \beta^2/2 = 1$, yields our maximal exponent on M to be $4 - 2\sqrt{3} - \epsilon$, where ϵ is a small positive number. We observe that $\rho = 4 - 2\sqrt{3} \approx 0.54$. Thus, for the appropriate growth rates on L and M ($L/M^\rho < c < 1$), the mean of the L^{th} largest noise variable dominates over the mean of the largest signal variable. To clarify the comparison, see Fig. 2.

We assume the required conditions above, and form a new random variable $D_{M,L} = S_{L:M-L} - B_{1:L}^{(\text{ud})}$. As the signal and noise variables are independent, we can determine that $\mathbf{E}[D_{M,L}] = \mathbf{E}_{L:M-L} - \mathbf{E}_{1:L}^{(\text{ud})}$ and $\text{var}[D_{M,L}] = \text{var}_{L:M-L} + \text{var}_{1:L}^{(\text{ud})}$. Furthermore, $\mathbf{E}[D_{M,L}] \xrightarrow{M,L \rightarrow \infty} \infty$ and $\text{var}[D_{M,L}] \xrightarrow{M,L \rightarrow \infty} 0$. From the Chebyshev inequality, we can show

$$\begin{aligned} &\Rightarrow \lim_{M,L \rightarrow \infty} P[|D_{M,L} - \mathbf{E}[D_{M,L}]| < \epsilon] \\ &\geq 1 - \lim_{M,L \rightarrow \infty} \frac{\text{var}[D_{M,L}]}{\epsilon^2} = 1. \end{aligned} \quad (45)$$

In the limit of large M and L , this difference variable approaches its mean with probability 1; recall that this mean value is infinity. Thus, the limiting distribution of the difference variable, $D_{M,L}$ is a delta function. Fatou's theorem enables the interchange of limits and integration, and we determine that

$$\lim_{M,L \rightarrow \infty} P[D_{M,L} > 0] = \lim_{M,L \rightarrow \infty} P[S_{L:M-L} > B_{1:L}^{(\text{ud})}] = 1. \quad \blacksquare$$

Thus, we note that for any rate of growth of multipath L that is less than M^ρ , we cannot acquire the multipath delay profile or any of the paths.

B. Random Path Amplitudes

Recall that our maximum likelihood detector considers the ordered absolute values of the observations. We first provide a result for the original observations (without taking the absolute value).

Theorem 2: (ur) case. Consider M independent, Gaussian random variables with the following distributions:

$$Y_i^{(\text{ur})} \sim \mathcal{N}\left(0, k \frac{\log M}{L} + 1\right), \quad i = 1, 2, \dots, L \quad (46)$$

$$Z_i \sim \mathcal{N}(0, 1), \quad i = 1, 2, \dots, M - L \quad (47)$$

where k is a constant that does not depend on L or M ; $L \leq M/3$.

We order the $Y_i^{(\text{ur})}$ such that $B_{1:L}^{(\text{ur})} = \max Y_i^{(\text{ur})}$ and $B_{L:L}^{(\text{ur})} = \min Y_i^{(\text{ur})}$; similarly, $S_{1:M-L} = \max Z_i$, $S_{M-L:M-L} = \min Z_i$ and $S_{L:M-L}$ is the L^{th} largest of $\{Z_i\}_{1}^{M-L}$. Then

$$\lim_{M,L \rightarrow \infty} P[S_{L:M-L} > B_{1:L}^{(\text{ur})}] = 1 \quad \text{if} \quad \frac{L}{M} \rightarrow 0. \quad (48)$$

Theorem 2 is proven in a manner similar to Theorem 1. The statistics of the largest signal variable after suitable approximation are,

$$\mathbf{E}_{1:L}^{(\text{ur})} \approx \sqrt{\frac{k \ln L \log M}{L} + 2 \ln L} \quad \text{and} \quad \text{var}_{1:L}^{(\text{ur})} \approx \frac{k \log M}{L \ln L}.$$

The decomposition required to show the dominance of the noise statistic over the signal statistic is somewhat different from that required in the deterministic case; however the principle is the same.

To complete the scenario of path detection for the Gaussian channel taps with uniform delay profile, we note that due to the fact that the observations are zero-mean under both cases (signal or noise only), the smallest signal variable, which is the most negative signal variable converges in distribution to the mean value $-\mathbf{E}_{1:L}^{(\text{ur})}$ with variance $\text{var}_{1:L}^{(\text{ur})}$.

Similarly the L^{th} smallest noise only statistic, which is also negative, converges in the mean to $-\mathbf{E}_{M-L:L}$. Thus, if we define $|S|_{L:M-L}$ as the L^{th} largest absolute noise statistic and $|B|_{1:L}^{(\text{ur})}$ as the largest absolute signal statistic, then $P[|S|_{L:M-L} > |B|_{1:L}^{(\text{ur})}] \xrightarrow{M,L \rightarrow \infty} 1$ for the conditions as stated in Theorem 2 above.

V. EXPONENTIAL PROFILE

We begin by further characterizing the exponential profile scenario. Our results for the exponential profile cases are based on analyzing a related uniform profile scenario, over which performance is superior to the exponential profile; thus, by showing for this modified uniform profile case that the noise dominates in the limit of large bandwidth, we conclude that the noise also dominates in the exponential profile case. As we shall see in the simulation results (Fig. 3), the acquisition of a channel with an exponential profile is not possible for a larger class of channels than Theorems 3 and 4 describe.

A. Deterministic Path Amplitudes

First, we consider the deterministic, exponential profile channel. We plug in the value for the channel normalization factor, $F^{(\text{e})}$, and also specify the strongest path (for delay $d_1 = 1$)

$$\begin{aligned} g^{(\text{ed})}(d_i) &= \sqrt{k_3 \frac{M}{L} (1 - e^{-2/M T_d \tau})} e^{-(d_i-1)/M T_d \tau} \\ \text{and } g_{\text{max}}^{(\text{ed})} &= \sqrt{k_3 \frac{M}{L} (1 - e^{-2/M T_d \tau})}. \end{aligned} \quad (49)$$

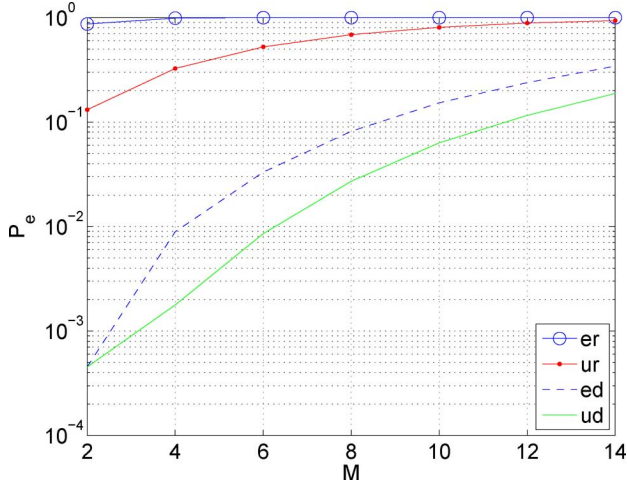


Fig. 3. Simulation results (probability of error) of ML acquisition with $M = 2L$. The plotted results are the average error of (12) and (15). The SNR is set at 15 dB and the flash parameter is set at $\theta = 1/\ln M$.

As means of calculating a lower bound on the penalty of error in channel acquisition we consider a uniform profile channel where all paths have $g(d_l) = g_{\max}^{(\text{ed})}$.

The probability of acquisition for the deterministic scenarios is determined by the set of distances, $\|\underline{s}_q^{(0)} - \underline{s}_l^{(0)}\|^2, q \neq l$; this collection is termed the distance spectrum. It is straightforward to show that the distance spectrum of this uniform profile is superior to the original exponential profile – basically this is due to the increased energy in each active tap along with the specific model for the delay profile that we employ. Thus, detection of the L strongest paths of the uniform profile affords an improved probability of acquisition versus the original (ed) profile.

We provide, without proof, the result for the new uniform profile case for deterministic channels. The proof is very similar to that of Theorem 1. The modifications of the proof are due to the fact that $g_{\max}^{(\text{ed})}$ is a function of both M and L .

Theorem 3: (ed) case. Consider M independent, Gaussian random variables with the following distributions:

$$\tilde{Y}_i^{(\text{ed})} \sim \mathcal{N}\left(\sqrt{k \frac{M \log M (1 - e^{-2/M T_d/\tau})}{L}}, 1\right),$$

$$i = 1, 2, \dots, L \quad (50)$$

$$Z_i \sim \mathcal{N}(0, 1), i = 1, 2, \dots, M - L \quad (51)$$

where k is a constant that does not depend on L or M ; $L \leq M/3$.

We order the $\tilde{Y}_i^{(\text{ed})}$ such that $B_{1:L}^{(\text{ed})} = \max \tilde{Y}_i^{(\text{ed})}$ and $B_{L:L}^{(\text{ed})} = \min \tilde{Y}_i^{(\text{ed})}$; similarly, $S_{1:M-L} = \max Z_i$, $S_{M-L:M-L} = \min Z_i$ and $S_{L:M-L}$ is the L^{th} largest of $\{Z_i\}_1^{M-L}$. Then

$$\lim_{M, L \rightarrow \infty} P\left[S_{L:M-L} > B_{1:L}^{(\text{ed})}\right] = 1 \text{ if } \frac{L}{M\rho} < c$$

$$\text{where } \rho = 4 - 2\sqrt{3}$$

$$\text{and } c < 1 \text{ is a constant.} \quad (52)$$

B. Random Path Amplitudes

We next consider random, exponential channels. As in the uniform case (ur), we first focus on the signed, ordered observation statistics. We look at a virtual uniform random profile scenario which achieves performance superior to that of the exponential random case and show that even over this new channel, the communication system fails to acquire in the limit of large bandwidth. Our new uniform profile has Gaussian i.i.d. amplitudes, that are equivalent to the strongest possible tap of the original exponential random profile. Thus, we look at the strongest path of the exponential profile at delay $d_1 = 1$ and get from (6)

$$g_{\max}^{(\text{er})} \sim \mathcal{N}\left(0, \frac{F^{(\text{e})^2}}{L} e^{-2/W\tau}\right) \sim \mathcal{N}\left(0, \frac{M}{L} \frac{1 - e^{-2T_d/M\tau}}{1 - e^{-2T_d/\tau}}\right). \quad (53)$$

Theorem 4: (er) case. Consider M independent, Gaussian random variables with the following distributions:

$$\tilde{Y}_i^{(\text{er})} \sim \mathcal{N}\left(0, k \frac{M \log M (1 - e^{-2T_d/M\tau})}{L} + 1\right),$$

$$i = 1, 2, \dots, L \quad (54)$$

$$Z_i \sim \mathcal{N}(0, 1), i = 1, 2, \dots, M - L \quad (55)$$

where k is a constant that does not depend on L or M ; $L \leq M/3$.

We order the $\tilde{Y}_i^{(\text{er})}$ such that $B_{1:L}^{(\text{er})} = \max \tilde{Y}_i^{(\text{er})}$ and $B_{L:L}^{(\text{er})} = \min \tilde{Y}_i^{(\text{er})}$; similarly, $S_{1:M-L} = \max Z_i$, $S_{M-L:M-L} = \min Z_i$ and $S_{L:M-L}$ is the L^{th} largest of $\{Z_i\}_1^{M-L}$. Then

$$\lim_{M, L \rightarrow \infty} P\left[S_{L:M-L} > B_{1:L}^{(\text{er})}\right] = 1$$

$$\text{if } \frac{L}{M} \rightarrow 0. \quad (56)$$

Proof: We first determine the statistics of the largest signal position. We use (18) and (19) again, with $G = L$ random variables, and examine the largest variable, that is $\nu = 1$. Recall that $m = 0$ and $\sigma = \sqrt{k(M \log M (1 - e^{-2T_d/M\tau})/L) + 1}$.

In the sequel, the variables k_4, k_5, k_6 and k_7 are constants which do not depend on the bandwidth. Taking L such i.i.d. variables, the largest has mean

$$\mathbf{E}_{1:L}^{(\text{er})} = \sqrt{k_4 \frac{M \log M (1 - e^{-2T_d/M\tau})}{L} + 1}$$

$$\left(\sqrt{2 \ln L} - \frac{\ln \ln L + \ln 4\pi - 2C}{2\sqrt{2 \ln L}} + O\left(\frac{1}{\ln L}\right)\right) \quad (57)$$

and variance

$$\mathbf{var}_{1:L}^{(\text{er})} = \frac{1}{2 \ln L} \left(k_4 \frac{M \log M (1 - e^{-2T_d/M\tau})}{L} + 1\right) \frac{\pi^2}{6}$$

$$+ O\left(\frac{1}{\ln^2 L}\right). \quad (58)$$

For a large bandwidth and a large number of paths, we get

$$\mathbf{E}_{1:L}^{(\text{er})} \approx \sqrt{k_6 \ln L \left(\frac{\log M}{L} + k_7 \right)} \quad (59)$$

$$\text{var}_{1:L}^{(\text{er})} \approx k_5 \frac{\log M}{L \ln L}. \quad (60)$$

Now we wish to compare $\mathbf{E}_{L:M-L}$ and $\mathbf{E}_{1:L}^{(\text{er})}$. We manipulate (28) and (59) and proceed with a decomposition as before, as shown below. The positive constants δ and η are not functions of M and L satisfy $\delta + \eta = 1$. We seek the conditions for the following inequality, in the limit of large L and M :

$$(\delta + \eta) \sqrt{2 \ln(M-L)} \gg ? \sqrt{k_6 \ln L \left(\frac{\log M}{L} + k_7 \right)} + \frac{\ln L}{\sqrt{2 \ln(M-L)}}. \quad (61)$$

We next follow steps similar to Section IV-A. The first term of (61)

$$\delta \sqrt{2 \ln(M-L)} \gg ? \sqrt{k_6 \ln L \left(\frac{\log M}{L} + k_7 \right)} \quad (62)$$

$$\delta^2 2 \ln(M-L) \gg ? k_6 \ln L \left(\frac{\log M}{L} + k_7 \right) \quad (63)$$

and (63) holds in the limit for any positive δ if $L/M \rightarrow 0$.

The second part of (61):

$$\begin{aligned} \eta \sqrt{2 \ln(M-L)} &\gg ? \frac{\ln L}{\sqrt{2 \ln(M-L)}} \\ \eta \ln(M-L) &\gg ? \ln L \rightarrow \\ (M-L)^{2\eta} &\gg ? L \end{aligned} \quad (64)$$

and this holds for $\eta > 1/2$.

Summarizing the conditions for (61), we need to determine δ and η such that (a) $\delta + \eta = 1$, (b) $\delta > 0$ and (c) $\eta > 1/2$. Any choice of $\eta > 1/2$ ensures that for any rate of increase for L , as long as it diverges more slowly than the bandwidth, the mean of the L^{th} largest noise variable dominates over the mean of the largest signal variable. Note that in our model, the number of multipath L cannot increase faster than the bandwidth, thus the fastest possible increase of L is $L \sim M$. The relationships between the strongest signal and the L^{th} noise are illustrated in Fig. 4.

Considering the negative paths, the situation is symmetric: the mean of the smallest (most negative) signal variable is higher than the the L^{th} most negative noise variable. To complete the proof, note that the L^{th} noise variable converges to its mean $\mathbf{E}_{L:M-L}$ because its variance diminishes. This mean dominates over the mean of the largest signal variable $\mathbf{E}_{1:L}^{(\text{er})}$, and over any constant multiple of it, in particular $2\mathbf{E}_{1:L}^{(\text{er})}$. We proceed to show that the probability of the largest signal variable exceeding $2\mathbf{E}_{1:L}^{(\text{er})}$ diminishes even though its variance may diverge (recall that $\text{var}_{1:L}^{(\text{er})} \approx k_5(\log M/L \ln L)$).

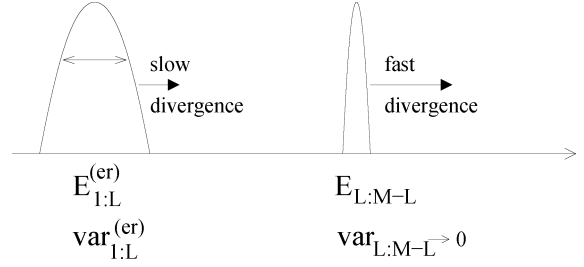


Fig. 4. Illustration of the distribution of the strongest signal position in the uniform PDP designed to bound performance over the exponential PDP with random amplitudes (er), and the L^{th} strongest noise position. Note that the noise variance diminishes while the strongest signal variance may diverge slowly. The mean of the L^{th} noise diverges faster than the mean of the strongest signal.

Recall that $B_{1:L}^{(\text{er})}$ is the largest signal variable. We have

$$\begin{aligned} \text{Prob} \left[\left| B_{1:L}^{(\text{er})} - \mathbf{E}_{1:L}^{(\text{er})} \right| \geq \mathbf{E}_{1:L}^{(\text{er})} \right] &= \\ \text{Prob} \left[B_{1:L}^{(\text{er})} \leq 0 \text{ or } B_{1:L}^{(\text{er})} \geq 2\mathbf{E}_{1:L}^{(\text{er})} \right] &\approx \\ \text{Prob} \left[B_{1:L}^{(\text{er})} \geq 2\mathbf{E}_{1:L}^{(\text{er})} \right]. \end{aligned} \quad (65)$$

Apply the Chebyshev inequality to (65) to get

$$\text{Prob} \left[B_{1:L}^{(\text{er})} \geq 2\mathbf{E}_{1:L}^{(\text{er})} \right] \leq \frac{\text{var}_{1:L}^{(\text{er})}}{\mathbf{E}_{1:L}^{(\text{er})^2}}.$$

Simple manipulation yields

$$\begin{aligned} \lim_{L,M \rightarrow \infty} \text{Prob} \left[B_{1:L}^{(\text{er})} \geq 2\mathbf{E}_{1:L}^{(\text{er})} \right] &\leq \\ \lim_{L,M \rightarrow \infty} \frac{k_5 \log M}{k_6 \log M \ln^2 L + k_4 L \ln^2 L} &= 0. \end{aligned}$$

Thus, we can conclude that

$$\lim_{L,M \rightarrow \infty} P \left[S_{L:M-L} > B_{1:L}^{(\text{er})} \right] = 1 \text{ if } \frac{L}{M} \rightarrow 0.$$

And the desired result is shown. \blacksquare

VI. CONCLUSION

To concretely show the effects of increasing bandwidth, we provide results of a small scale simulation. Fig. 3 shows the probability of acquisition for maximum likelihood detection for the four scenarios considered herein. We assume that $M = 2L$ and thus a less restrictive case is examined than dictated by our theorems. We simulate an environment where the SNR is 15 dB. Our theorems state that as the number of noise positions outnumber that of the signal positions, acquisition becomes more challenging. Due to this result, the exponential profiles yield worse performance than the uniform profiles due to the presence of more signal positions with relatively low signal energy in the exponential profiles. In addition, as to be expected, energy detection for random signals yields performance inferior to correlation detection for deterministic signals. These trends are clearly displayed in Fig. 3.

In this work, we have considered the problem of multipath delay profile acquisition for the PPM modulation in ultra wideband communication systems. Even under the idealized conditions of no inter-symbol interference and perfect knowledge of the transmitted symbols and channel gains, the optimal acquisition algorithm fails in the limit of large bandwidth if the number of paths diverges, but is sublinear with respect to bandwidth. We have considered four types of channels based on deterministic or Gaussian channel gains and uniform or exponential power delay profiles. The failure condition for the deterministic channel gains is $L < W^\rho$ where $\rho \approx 1/2$; whereas for the Gaussian power delay profiles, we need $L/W \rightarrow 0$. Any slower rate of growth on the multipath with respect to bandwidth will also lead to a failure of acquisition due to the relative increase in channel uncertainty.

Our results indicate that the achievable rate of synchronous PPM systems over rich multipath channels diminishes as the bandwidth increases. The underlying reason is the low spectral efficiency of the PPM modulation that allows it only moderate peakiness, namely its bursts of transmission cannot be very energetic. PPM is an orthogonal modulation, thus its spectral efficiency depends on bandwidth via $\log W/W$. In order to maintain a high data rate as the bandwidth increases, the PPM system must become more and more peaky, in other words it must be “flashy” [34]. However, the low spectral efficiency does not allow the PPM system to concentrate a lot of data per transmitted burst. Thus, the system is forced to transmit frequent bursts of signal. The system is power limited, thus each of these bursts of communication cannot be too strong. As the bandwidth increases, the bursts of signal gradually sink into the noise, until, in the limit, acquisition becomes impossible.

APPENDIX DERIVATION OF UNIFORM RANDOM CHANNEL EQUIVALENT ML DETECTOR

Considering the uniform random channel gain case, recall from (16) that we have

$$\begin{aligned} \arg \max p(\underline{Y}(\mathbf{ur})|H_q) &= \arg \min \underline{Y}(\mathbf{ur})^T C_q(\mathbf{ur})^{-1} \underline{Y}(\mathbf{ur}) \\ &= \arg \min \tilde{c}_q^T \underline{Y}(\mathbf{ur})^2 \end{aligned}$$

where $\underline{Y}(\mathbf{ur})^2 = \underline{Y}(\mathbf{ur}) \odot \underline{Y}(\mathbf{ur})$, and \odot denotes the Schur product (component-wise multiplication). Since $C_q(\mathbf{ur})^{-1}$ is diagonal, the vector \tilde{c}_q contains the diagonal elements of $C_q(\mathbf{ur})^{-1}$, where its i^{th} element is

$$\tilde{c}_q(i) = \begin{cases} 1, & \text{if } p_q(i) = 0 \\ \frac{1}{1 + \frac{\varepsilon}{L\theta}} = 1 - \frac{\varepsilon}{1 + \frac{\varepsilon}{L\theta}}, & \text{if } p_q(i) = 1 \end{cases}$$

$i = 1, 2, \dots, M.$

Thus, $\tilde{c}_q = \mathbf{1} - \kappa p_q$, where $\kappa = (\varepsilon/L\theta)/(1 + \varepsilon/L\theta) > 0$. Recall that p_q is the multipath location vector and that its components are either zero or unit valued. Then

$$\begin{aligned} \arg \min \tilde{c}_q^T \underline{Y}(\mathbf{ur})^2 &= \arg \min \mathbf{1}^T \underline{Y}(\mathbf{ur})^2 - \kappa p_q^T \underline{Y}(\mathbf{ur})^2 \\ &= \arg \min -\kappa p_q^T \underline{Y}(\mathbf{ur})^2 \\ &= \arg \max p_q^T \underline{Y}(\mathbf{ur})^2 \quad \text{since } \kappa > 0. \end{aligned}$$

Let $\hat{q}(\mathbf{ur}) = \arg \max_q p_q^T \underline{Y}(\mathbf{ur})^2$. Given the arguments employed to show (14), for any $q \neq \hat{q}(\mathbf{ur})$ we can order the components of $\underline{Y}(\mathbf{ur})^2$ which contribute to $p_q^T \underline{Y}(\mathbf{ur})^2$. The ordered components corresponding to $\hat{q}(\mathbf{ur})$ dominate over the ordered components of any other q , and thus we have that

$$\arg \max_q p_q^T \underline{Y}(\mathbf{ur})^2 = \arg \max_q p_q^T |\underline{Y}(\mathbf{ur})|.$$

ACKNOWLEDGMENT

The authors thank A. Samorodnitsky for his participation and help on statistical matters.

REFERENCES

- [1] S. Aedudodla, S. Vijayakumaran, and T. F. Wong, Timing Acquisition in Ultra-Wideband Communication Systems 2005 [Online]. Available: <http://www.wireless.ece.ufl.edu/twong/Preprints/uwbacqvt.pdf>
- [2] J. Cai, X. Shen, J. W. Mark, H. Liu, and T. D. Todd, “Semiblind channel estimation for pulse-based ultra-wideband wireless communication systems,” *IEEE Trans. Veh. Technol.*, vol. 55, no. 1, pp. 95–103, Jan. 2006.
- [3] C. Carbonelli and U. Mitra, “Clustered ML channel estimation for ultra-wideband signals,” *IEEE Trans. Wireless Commun.*, Dec. 2006, to be published.
- [4] C. Carbonelli, S. Vedantam, and U. Mitra, “Sparse channel estimation with zero-tap estimation,” *IEEE Trans. Wireless Commun.*, vol. 6, no. 5, pp. 1743–1763, May 2007.
- [5] L.-C. Chu and U. Mitra, “Performance analysis of the improved MMSE multi-user receiver for mismatched delay channels,” *IEEE Trans. Commun.*, vol. 46, no. 10, pp. 1369–1380, Oct. 1998.
- [6] H. Cramér, *Mathematical Methods of Statistics*. Princeton, NJ: Princeton University Press, 1946.
- [7] R. J. Cramer, R. A. Scholtz, and M. Z. Win, “Evaluation of an ultra-wide-band propagation channel,” *IEEE Trans. Antennas Propag.*, vol. 50, no. 5, pp. 561–570, May 2002.
- [8] G. Durisi and S. Benedetto, “Performance of coherent and non coherent receivers for UWB communications,” in *Proc. IEEE Int. Conf. Communications*, Jun. 2004, vol. 6, pp. 3429–3433.
- [9] J. L. Richards et al., “System for Fast Lock and Acquisition of Ultra-Wideband Signals,” U.S. Patent 6 556 621, Apr. 2003.
- [10] J. Foerster, Channel Modeling Sub-Committee Report Final 2003, Final Report IEEE P802.15 02/490r1 SG3a.
- [11] S. Franz, C. Carbonelli, and U. Mitra, “Semi-blind ml synchronization for UWB systems,” *IEEE Trans. Wireless Commun.*, 2007, to be published.
- [12] R. G. Gallager, *Information Theory and Reliable Communication*. New York: Wiley, 1968, sec. 8.6.
- [13] S. Gezici, E. Fishler, H. Kobayashi, and H. V. Poor, “A rapid acquisition technique for impulse radio,” in *Proc. Pacific Rim Conf. Communications, Computers and Signal Processing (PACRIM)*, Aug. 2003.
- [14] K. Haneda, J.-I. Takada, and T. Kobayashi, “A parametric UWB propagation channel estimation and its performance validation in an anechoic chamber,” *IEEE Trans. Microwave Theory Tech.*, vol. 54, no. 4, pp. 1802–1811, Jun. 2006.
- [15] E. A. Homier and R. A. Scholtz, “Rapid acquisition of ultra-wideband signals in the dense multipath channel,” in *Proc. Conf. Ultra Wideband Systems and Technologies*, 2002.

- [16] N. L. Johnson and S. Kotz, *Continuous Univariate Distributions – I*. New York: Houghton Mifflin, 1970.
- [17] R. S. Kennedy, *Fading Dispersive Communication Channels*. New York: Wiley, 1969.
- [18] P. Liu and Z. Xu, “POR-based channel estimation for UWB communications,” *IEEE Trans. Wireless Commun.*, vol. 4, no. 16, pp. 2968–2982, Nov. 2005.
- [19] W. M. Lovelace and J. K. Townsend, “The effects of timing jitter on the performance of impulse radio,” *IEEE J. Select. Areas Commun.*, vol. 20, no. 9, pp. 1646–1651, Dec. 2002.
- [20] M. Médard and R. G. Gallager, “Bandwidth scaling for fading multipath channels,” *IEEE Trans. Inf. Theory*, vol. 2002, pp. 840–852, Apr. 2002.
- [21] M. Pendergrass, Empirically Based Statistical Ultra-Wideband Model IEEE 802.15 Working Group for Wireless Area Networks (WPANs), 2002, Contribution 02/240.
- [22] D. Porrat and U. Mitra, “On synchronization of wideband impulsive systems in multipath,” in *Proc. IEEE ISIT*, Sep. 2005.
- [23] D. Porrat, D. N. C. Tse, and S. Nacu, “Channel uncertainty in ultra wideband communication systems,” *IEEE Trans. Inf. Theory*, vol. 53, no. 1, pp. 194–208, Jan. 2007.
- [24] J. G. Proakis, *Digital Communications*, 4th ed. New York: McGraw-Hill, 2000.
- [25] R. C. Qiu, “A study of the ultra-wideband wireless propagation channel and optimum UWB receiver design,” *IEEE J. Select. Areas Commun.*, vol. 20, pp. 1628–1637, Dec. 2002.
- [26] R. C. Qiu, “A generalized time domain multipath channel and its application in ultra-wideband (UWB) wireless optimal receiver design: System performance analysis,” in *Proc. IEEE Int. Conf. Wireless Communications and Networking*, Mar. 2004, vol. 2, pp. 901–907.
- [27] L. Rusch, C. Prettie, D. Cheung, Q. Li, and M. Ho, “Characterization of UWB propagation from 2 to 8 GHz in a residential environment,” *IEEE J. Select Areas Commun.*
- [28] R. Saadane, A. Menouni, R. Knopp, and D. Aboutajdine, “Empirical eigenanalysis of indoor UWB propagation channels,” in *Proc. IEEE Globecom*, Oct. 2004, vol. 5, pp. 3215–3219.
- [29] U. Schuster and H. Bölcskei, “Ultra-wideband channel modeling on the basis of information-theoretic criteria,” *IEEE J. Select Areas Commun.*, 2005, submitted for publication.
- [30] Y. Souilmi and R. Knopp, “On the achievable rates of ultra-wideband PPM with non-coherent detection in multipath environments,” in *Proc. IEEE Int. Conf. Communications (ICC’03)*, May 2003.
- [31] V. G. Subramanian and B. Hajek, “Broad-band fading channels: Signal burstiness and capacity,” *IEEE Trans. Inf. Theory*, vol. 48, no. 4, pp. 809–827, Apr. 2002.
- [32] I. E. Telatar and D. N. C. Tse, “Capacity and mutual information of wideband multipath fading channels,” *IEEE Trans. Inf. Theory*, vol. 46, no. 7, pp. 1384–1400, Jul. 2000.
- [33] Z. Tian and G. B. Giannakis, “BER sensitivity to mis-timing in correlation-based UWB receivers,” in *Proc. IEEE Globecom*, San Francisco, CA.
- [34] S. Verdú, “Spectral efficiency in the wideband regime,” *IEEE Trans. Inf. Theory*, vol. 48, no. 6, pp. 1319–1343, Jun. 2002.
- [35] S. Vijayakumaran, T. F. Wong, and S. Aedudodla, “On the asymptotic performance of threshold-based acquisition systems in multipath fading channels,” in *Proc. IEEE Information Theory Workshop*, Oct. 2004.
- [36] M. Z. Win and R. A. Scholtz, “Characterization of ultra-wide bandwidth wireless communications channels: A communication theoretic view,” *IEEE J. Selected Areas Commun.*, vol. 20, no. 9, pp. 1613–1627, Dec. 2002.
- [37] L. Yang, “Timing PPM-UWB signals in ad hoc multi-access,” *IEEE J. Selected Areas Commun.*, 2006, to be published.
- [38] F. Zhu, Z. Wu, and C. R. Nassar, “Generalized fading channel model with application to UWB,” in *Proc. UWBST 2002*, May 2002, pp. 13–17.



Dana Porrat (M’05) received the Ph.D. degree from Stanford University, Stanford, CA, in 2002.

She is a Lecturer in the Engineering and Computer Science School, Hebrew University, Jerusalem, Israel, and Head of the Wideband Radio Communications Laboratory. Her research interests include stability aspects of radio propagation over very wide bandwidths and information-theoretic aspects of radio communications, in particular the effect of channel uncertainty on systems.

Urbashi Mitra (F’07) received the B.S. and the M.S. degrees from the University of California at Berkeley in 1987 and 1989, respectively, both in electrical engineering and computer science, and the Ph.D. degree in electrical engineering from Princeton University, Princeton, NJ, in 1994.

From 1989 to 1990 she was a Member of Technical Staff at Bellcore, Red Bank, NJ. From 1994 to 2000, she was a faculty member of the Department of Electrical Engineering, The Ohio State University, Columbus. In 2001, she joined the Department of Electrical Engineering, University of Southern California at Los Angeles, where she is currently a Professor. She has held visiting appointments at the Eurecom Institute, Rice University, and Stanford University. She is currently the co-Director of the Communication Sciences Institute at the University of Southern California.

Dr. Mitra is an Associate Editor for the IEEE TRANSACTIONS ON INFORMATION THEORY and the IEEE JOURNAL OF OCEANIC ENGINEERING. She was an Associate Editor for the IEEE TRANSACTIONS ON COMMUNICATIONS from 1996 to 2001. She is serving a second term as a member of the IEEE Information Theory Society’s Board of Governors. She is the recipient of: Texas Instruments Visiting Professor (Fall 2002, Rice University), 2001 Okawa Foundation Award, 2000 Lumley Award for Research (OSU College of Engineering), 1997 MacQuigg Award for Teaching (OSU College of Engineering), 1996 National Science Foundation (NSF) CAREER Award, 1994 NSF International Postdoctoral Fellowship, 1998 Lockheed Leadership Fellowship, 1987 California Microelectronics Fellowship. She has co-chaired the IEEE Communication Theory Symposium at ICC 2003 in Anchorage, AK and the first ACM Workshop on Underwater Networks at Mobicom 2006, Los Angeles, CA. She is currently the tutorials Chair for IEEE ISIT 2007 in Nice, France, and Finance Chair for IEEE ICASSP 2008 in Las Vegas, NV.